Pharmaceutical Research, Vol. 25, No. 3, March 2008 (© 2007)
DOI: 10.1007/s11095-007-9410-5

Research Paper

Delivery by Cationic Gelatin Nanoparticles Strongly Increases the Immunostimulatory Effects of CpG Oligonucleotides

Klaus Zwiorek,[1] Carole Bourquin,[2] Julia Battiany,[2] Gerhard Winter,[1] Stefan Endres,[2] Gunther Hartmann,[3] and Conrad Coester[1,4]

Received February 26, 2007; accepted July 10, 2007; published online October 3, 2007

Purpose. Cationized gelatin nanoparticles (GNPs) were used as carrier to improve delivery of immunostimulatory CpG oligonucleotides (CpG ODN) both *in vitro* and *in vivo*.
Methods. Uptake of CpG ODN-loaded cationized gelatin nanoparticles (CpG-GNPs) into murine myeloid dendritic cells (DCs) and their respective immunostimulatory activity was monitored. *In vivo*, induction of cytokine secretion by CpG-GNPs was measured. For experiments on primary human cells, prototypes of the three CpG ODN classes were adsorbed onto GNPs. Uptake and induction of proinflammatory cytokines were assessed in human plasmacytoid DCs and B cells, the only existing human target cells for CpG ODN.
Results. In the murine system, gelatin nanoparticle formulations enhanced the uptake and immunostimulatory activity of CpG ODN both *in vitro* and *in vivo*. Furthermore, delivery by cationized gelatin nanoparticles of CpG ODN of the classes B and C to primary human plasmacytoid DCs increased production of IFN-α, a key cytokine in the driving of both the innate and adaptive immune responses.
Conclusion. GNPs can be used as a biodegradable and well tolerated carrier to deliver CpG ODN to their target cells and strongly increase activation of the immune system. This concept may be applied as novel adjuvant for antiviral and antitumoral vaccines.

KEY WORDS: adjuvant; B cells; CpG oligonucleotide; dendritic cells; gelatin nanoparticles.

INTRODUCTION

Specific patterns within the microbial DNA are responsible for the recognition of viral and bacterial pathogens by the vertebrate immune system. In particular, DNA rich in unmethylated cytidine–guanosine dinucleotides (CpG motifs), is sensed as the key danger signal. CpG motifs are detected in the endosome of antigen presenting cells by the pattern recognition receptor Toll-like receptor 9. Thus, it is well established that binding of synthetic oligodeoxynucleotides containing CpG motifs (CpG ODN) to Toll-like receptor 9 enhances the generation of an innate immune response and promotes protective T_H1-type immunity in animal models (1). In humans, clinical studies have demonstrated a strong potential for CpG ODN as adjuvant in antiviral vaccination, cancer and treatment of asthma and other allergic diseases (reviewed in (1)).

Several particulate (2–6) and liposomal (7, 8) delivery approaches for CpG ODN have been developed to enhance the immunostimulatory efficacy. For instance, enhanced immunological activity of CpG ODN is observed after incorporation into the matrix of biodegradable poly(D,L-lactic-co-glycolide acid) (PLGA) nanoparticles (2, 3). Furthermore, very promising results were achieved using cationized poly (lactide-co-glycolide) (PLG) microparticles and adsorbing CpG ODN by electrostatic interactions on the particle surface (6). The advantage of this system is the direct presentation of CpG ODNs on the carrier that may result in a more rapid activation than with carrier-incorporated CpG ODN, since no diffusion or particle degradation is necessary before the ODN can interact with the receptor.

Early studies revealed species-specific differences in the optimal CpG motif. Whereas GACGTT was determined as the optimal CpG motif to activate the immune system of mice (9), GTCGTT optimally stimulates nonhuman primate and human cells (10). Moreover, the cell types that express the Toll-like receptor 9 differ between species. In mice, Toll-like receptor 9 is expressed in cells of the myeloid lineage such as myeloid dendritic cells (DCs) as well as on B cells and plasmacytoid DCs. In humans, the receptor is exclusively expressed in plasmacytoid DCs and B cells (11). These species-specific differences highlight the importance of

[1] Department of Pharmacy, Pharmaceutical Technology and Biopharmaceutics, Ludwig-Maximilians-University, Butenandtstr. 5-13, 81377, Munich, Germany.
[2] Department of Internal Medicine, Division of Clinical Pharmacology, Ludwig-Maximilians-University, Ziemssenstr. 1, 80336, Munich, Germany.
[3] Department of Internal Medicine, Division of Clinical Pharmacology, University of Bonn, Sigmund-Freud-Str. 25, 53127, Bonn, Germany.
[4] To whom correspondence should be addressed. (e-mail: conrad.coester@cup.uni-muenchen.de)

reproducing findings obtained in the murine system in human primary cell populations. In addition, three classes of CpG ODNs have been defined that differ in the quality of their immunostimulatory activity. CpG ODN binding to human Toll-like receptor 9 are defined as CpG ODN class A with its prototype ODN 2216 (CpG-A), CpG ODN class B with its prototype ODN 2006 (CpG-B), and the newly established CpG ODN class C with ODN M362 (CpG-C). CpG-A is known to stimulate the production of high amounts of IFN-α/β (type I interferons) in plasmacytoid DCs, but is weak in B cell activation. On the other hand, CpG-B ODN selectively activate plasmacytoid DCs and induce their maturation, but are unable to initiate the secretion of IFN-α/β. Moreover, CpG-B ODNs are able to activate B cells. The sequence prototype is ODN 2006 in the human system and ODN 1826 in the murine system (10). CpG-C is an intermediate between CpG-A and CpG-B that can activate the secretion of IFN-α in plasmacytoid DCs and the proliferation of B cells (12).

The goal of the present study was to investigate the potential of cationized gelatin nanoparticles as carrier for CpG ODN. Gelatin offers several advantages as a biomaterial for the preparation of colloidal drug carriers. Its protein structure provides sites for selective linking of various functionalities. Furthermore, the high physiological tolerance of gelatin, its biocompatibility, and its biodegradability are well established for years (13, 14). The US Food and Drug Administration (FDA) classified gelatin as "Generally Recognized as Safe" excipient and it is a constituent of various plasma expanders. The preparation of homogeneous colloidal spheres using the two-step desolvation technique is quite simple and reproducible (15). We have recently described the use of cationized gelatin nanoparticles as a highly potent and well tolerated plasmid DNA transfection system (16).

In this study, uptake and immunostimulatory activity of CpG ODN bound to cationized gelatin nanoparticles was studied in mouse myeloid dendritic cells. Dendritic cells are professional antigen presenting cells that are essential for the generation of protective immune responses against pathogens and tumors. Stimulation of DCs through CpG ODN activates intracellular signaling cascades that rapidly induce the expression of a variety of genes involved in maturation and migration of DCs. In addition to the study of CpG ODN-loaded gelatin nanoparticles in myeloid DC cultures, results were confirmed by *in vivo* application of these formulations. To assess stimulatory potential in human cells, uptake and activation was studied in human plasmacytoid DCs and B cells, the only human cell populations expressing Toll-like receptor 9 and therefore able to respond directly to CpG ODN.

MATERIAL AND METHODS

Materials

Gelatin type A from porcine skin (175 Bloom), glutaraldehyde (25%), acetone, 1-ethyl-3-(3-dimethyl-aminopropyl) carbodiimide hydrochloride (EDC) and (2-aminoethyl)-trimethylammoniumchloride hydrochloride (cholaminechloride hydrochloride) were purchased from Sigma-Aldrich GmbH (Taufkirchen, Germany). The sequences of the various utilized synthetic CpG ODNs and control ODNs that were obtained from Coley Pharmaceutical Group (Wellesley, MA, USA) are given in Table I. Tetramethylrhodamine conjugated dextran (mol. wt. 40000 Da) (TMR dextran), Texas Red-X™ succinimidyl ester, and the applied Alexa™ Fluor dyes were purchased from Invitrogen (Karlsruhe, Germany). Monoclonal antibodies specific for CD11c, CD86, MHC-II and their respective fluorescein isothiocyanate (FITC) conjugated secondary antibodies were purchased from BD Pharmingen (Mississauga, Canada). Granulocyte macrophage colony stimulating factor (GM-CSF) was purchased from PeproTech, Inc. (Rockville, USA). Fetal calf serum (FCS) came from GibcoBRL (Paisley, UK). L-Glutamine, penicilline, and streptomycine were purchased from PAA (Linz, Austria). RPMI-1640 medium was obtained from Biochrom AG (Berlin, Germany).

Preparation of Cationized Gelatin Nanoparticles

Gelatin nanoparticles were prepared according to the two-step desolvation method including further optimization (15). Briefly, 1.25 g gelatin was dissolved in 25 ml highly purified water (5% *w*/*w*) at 50°C under constant stirring (700 rpm). The first desolvation step was initiated by quick addition of 25 ml acetone. After discarding the supernatant containing low molecular weight fractions of gelatin, the sediment was redissolved in 25 ml water under constant stirring at 50°C. Dependent on the desired particle size, the pH was then adjusted to a value between 2.3 (approx .resulting particle size: 150 nm) and 3.0 (approx. resulting particle size: 300 nm). Subsequently, the second desolvation step was initiated by drop-wise addition of 50 ml acetone (during constant stirring at 700 rpm) and resulted in the formation of nanoparticles. The nanoparticles were stabilized by cross-linking with glutaraldehyde (150 µl of a 25% solution) under constant stirring. After 12 h the particles were purified from non-reacted glutaraldehyde by centrifugation and redispersion in highly purified water.

Cationization of the nanoparticles was achieved through introduction of a quaternary amino group by covalent coupling of cholaminechloride hydrochloride onto the particles' surface, as previously described for a gene delivery approach (16). Thereby, the aqueous dispersion of native nanoparticles was adjusted to pH 4.5 and a molar excess of the cationization agent (e.g. 50 mg per 500 mg nanoparticles) was added under constant stirring. After 5 min of incubation, a molar excess of EDC (50 mg) was added to activate free

Table I. Sequences of the Applied CpG ODNs

Name	Description
ODN 1826	Mouse specific CpG ODN 5′ TCCATGA*CG*TTCCTGA*CG*TT 3′[a]
ODN 1911	Control ODN 5′ TCCAGGACTTTCCTCAGGT 3′[a]
ODN 2006	Prototype CpG-B ODN 5′ T*CG*TT*CG*TTTTGT*CG*TTTTGT*CG*TT 3′[a]
ODN 2216	Prototype CpG-A ODN 5′ Ggggg*acgatcgtcG*GGGGGg 3′[a]
ODN M362	Prototype CpG-C ODN 5′ T*CGTCGTCGTTCG*AA*CGACG*TTGAT 3′[a]
ODN M383	GC pendant to ODN M362 5′ TGCTGCTGCTTGCAAGCAGCTTGAT 3′[a]

[a] *Capital letters* Nucleotides with phosphorothioated backbones, *others* phosphodiester backbones

carboxyl groups on the particles to react with cholamine. During the cationization reaction the primary amino group of cholamine could react with both, residual aldehyde groups derived from only mono-functionally bound cross-linking reagent glutaraldehyde, as well as the activated carboxyl groups on the nanoparticles surface. The reaction was stopped after 1 h and the nanoparticles were purified by threefold centrifugation and redispersion.

Some nanoparticle batches were additionally labeled with fluorescence dyes. This was either done by covalent linkage of 2 mg Texas Red-X to the redissolved gelatin solution after the first desolvation step (CLSM experiments) or encapsulation of 2 mg tetramethylrhodamine (TMR) conjugated dextran into the nanoparticle matrix (FACS experiments). Prior usage, a sample of fluorescence labeled nanoparticles was centrifuged and spectro-photometrically checked for the absence of free dye in the supernatant to exclude the presence of free unbound dye in the experiments.

Characterization of the Nanoparticles

The size of the prepared nanoparticles was measured by dynamic light scattering using a Zetasizer Nano ZS (Malvern, Worcestershire, UK). In addition, surface morphology of unloaded cationized gelatin nanoparticles was analyzed by scanning electron microscopy (Jeol, Ebersberg, Germany). Zeta potential (ζ potential) measurements were conducted in physiological PBS of pH 7.4 (conductivity: 16–17 mS/cm) with the Zetasizer Nano ZS (Malvern).

ODN Loading of Cationized Gelatin Nanoparticles

600 μg nanoparticles were incubated with 30 μg of ODN in 400 μl PBS of pH 7.4 for 30 min under gentle shaking at room temperature. The nanoparticle dispersion was then centrifuged and the supernatant was analyzed UV-spectrophotometrically at 260 nm wavelength for unbound ODN.

Cell Culture

Murine Myeloid Dendritic Cells (DCs)

Myeloid DCs were generated from murine bone marrow precursors following the method previously described by Lutz *et al.* (17). Briefly, 2×10^6 bone marrow cells obtained from the femurs of C57BL/6 mice were plated in bacteriological grade petri dishes in 10 ml of RPMI-1640 medium containing 20 ng/ml of GM-CSF (complete media) and incubated at 37°C and 5% CO_2. On day 3, the culture was supplemented with 10 ml of complete media and on day 6, half of the culture media was removed and replaced with fresh complete media. The purity of the semi-adherent and non-adherent DC populations on day 7 was found to be greater than 80% (based on the expression of CD11c). All compounds were purchased endotoxin-tested. Viability of isolated cells was determined by trypan-blue exclusion.

Primary Human Plasmacytoid DCs and B Cells

Human PBMCs (monocytes and lymphocytes) were isolated from buffy coats (leucocytes obtained by centrifugation from the whole blood) provided by the blood bank of the University of Greifswald, Germany. Blood donors were between 18 to 65 years old healthy women and men, which were tested to be negative for HIV, HBV, and HCV. Further exclusion criteria were manifest infections during the last 4 weeks, fever, symptomatic allergies, abnormal blood cell counts, increased liver enzymes or medication of any kind except vitamins and oral contraceptives. PBMCs were prepared from buffy coats by Ficoll-Hypaque density gradient centrifugation (Biochrom, Berlin, Germany).

Plasmacytoid DCs were isolated using an anti-BDCA-4 antibody according to the manufacturer's protocol (BDCA-4 Cell-Isolation-Kit, Miltenyi Biotec, Bergisch-Gladbach, Germany). The purity of the isolated DC cultures was 96–98% as assessed by flow cytometric analysis.

Purified B cells were obtained by using the CD19 B cell isolation kit from Miltenyi Biotec. Briefly, B cells were labeled with anti-CD19 antibody coupled to colloidal paramagnetic microbeads and passed through a magnetic separation column (LS, Miltenyi Biotec). The purity of isolated B cells was >95% as assessed by flow cytometric analysis with no plasmacytoid DCs detectable (<0.005%). The various isolated cells were resuspended in RPMI 1640 medium supplemented with 8% human AB-serum, 1.5 mM L-glutamine, 100 U/ml penicillin, and 100 μg/ml streptomycin. Cells were cultured in 96-well round bottom plates (200 μl medium/well; final concentration PBMCs: 2×10^6/ml, plasmacytoid DCs: 2.5×10^5/ml, B cells: 2×10^5/ml). All compounds were purchased endotoxin-tested. Viability of isolated cells was determined by trypan-blue exclusion.

FACS Analysis of Murine Myeloid DCs

Seven days old myeloid DCs were incubated for 12 hours with CpG ODN-loaded and fluorescence-labeled formulations (CpG-GNP004F) or unloaded fluorescence-labeled nanoparticles (GNP004F). After 12 h, the cells were harvested and washed thoroughly in cold staining buffer (PBS containing 10% FBS and 0.05% sodium azide) and transferred into FACS tubes. For phenotypic analysis of cells that have taken up the nanoparticles, surface staining was performed. Therefore, murine myeloid dendritic cells were labeled using a monoclonal antibody specific for CD11c together with an appropriate FITC-conjugated secondary antibody (along with an isotype control). To further investigate a potential DC maturation, additional experiments were performed, where cells were labeled with CD86 and MHC-II antibodies and appropriate FITC-conjugated secondary antibodies. The samples were analyzed using a FACsort. The events were collected by gating on the total live cell populations without further specific gating of particular subpopulations. A minimum of 10,000 events was collected.

CLSM Experiments with Murine Myeloid DCs and Primary Human Plasmacytoid DCs

Murine Myeloid DCs

4×10^5 of murine myeloid DCs were transferred into Lab-Tek II eight well chamber slides (Nalge Nunc International, Rochester, USA) and covered with 200 μl of medium.

DCs were incubated with 8 μg of CpG ODN-loaded Texas Red-X-labeled nanoparticles (GNP003F loaded with 400 ng of CpG ODN) in a final volume of 500 μl. Control wells were treated with the phagocytosis inhibitor Cytochalasin B (5 μg/ml) from 30 min prior to the addition of nanoparticles on.

After incubation for 8 h, the supernatant in the chamber slide cultures was carefully removed. The cells were washed thrice with PBS. Murine myeloid DCs were stained with a CD11c specific primary antibody followed by a FITC-labeled secondary antibody. After the final washing step, cells were fixed with 4% paraformaldehyde. Chamber slides were finally prepared with a solution of 2.5% DABCO and PBS/glycerol (1:1) and visualized under a Zeiss 510 LSM NLO confocal laser scanning microscope (Carl Zeiss Microscope Systems, Jena, Germany).

Primary Human Plasmacytoid DCs

Uptake experiments into human plasmacytoid DCs were performed with CpG ODNs that were previously labeled (3′terminal) with fluoresceine (Coley Pharmaceutical Group). 5×10^4 isolated plasmacytoid DCs in 200 μl of medium were transferred into Lab-Tek II eight well chamber slides (Nalge Nunc International). The medium additionally contained 2 ng IL-3.

The cells were incubated with 12 μg of fluorescence-labeled CpG-A ODN 2006-loaded cationized gelatin nanoparticles (containing 600 ng of CpG ODN). After incubation for 8 hours, the supernatant in the chamber slide cultures was carefully removed. The cells were washed thrice with PBS and stained with 100 μl of a 0.0005% Alexa Fluor™ 594 Concanavalin A solution in PBS for 1 min (unspecific cell membrane stainer). After a final washing step, cells were fixed with 4% paraformaldehyde. Chamber slides were finally prepared with a solution of 2.5% DABCO and PBS/glycerol (1:1) and visualized under the CLSM.

Cytokine Quantification by ELISA

Quantitative cytokine analysis for IL-6, IL-12p70, and TNF-α in the culture supernatant of myeloid DCs that were treated with CpG-GNPs or controls was performed using specific ELISA Ready-SET-Go kits (eBioscience Inc., San Diego, USA) according to the manufacturer's instructions (detection ranges: IL-6=4–500 pg/ml; IL-12p70=15–2,000 pg/ml; TNF- α=8–1,000 pg/ml). IFN-α secreted from plasmacytoid DCs was quantified with the IFN-α module set from Bender MedSystems (Vienna, Austria; detection range 8–500 pg/ml). This ELISA detects most of the IFN-α isoforms, except IFN-α B and IFN-α F. IL-6 on human B cells was measured by using the human IL-6 OptEIA ELISA (Bender Med Systems; detection range 4.7–300 pg/ml).

In vivo Experiments

Mice

Female Balb/c and C57BL/6 mice were purchased from Harlan-Winkelmann (Borchen, Germany). Mice were 5–12 weeks of age at the onset of experiments. Animal studies were approved by the local regulatory agency (Regierung von Oberbayern, Munich, Germany).

Immunostimulation via i.v. Injection

For *in vivo* immunostimulation, 500 μg cationized gelatin nanoparticles were incubated with 50 μg of oligonucleotides and 100 μl PBS for 20 min and injected i.v. into the retroorbital plexus. Blood samples were obtained 18 h post injection by retroorbital puncture. Serum was prepared by centrifugation and stored at −20°C.

Gelatin-specific Immune Response

To assess a possible immune response to gelatin, mice were immunized twice s.c. at a 14-day interval with 2 mg cationized gelatin nanoparticles loaded with 100 μg CpG 1826. As positive control, one group of mice was immunized s.c. with 50 μg gelatin in complete Freund's adjuvant and boosted 14 days later with 100 μg gelatin in incomplete Freund's adjuvant. Seven days after the second immunization, serum samples were prepared. Serum antibodies to gelatin were determined by ELISA: 96-well plates were coated overnight with 10 μg/ml gelatin in PBS and blocked 1 h with 1% BSA in PBS. After incubation of serum samples for 1 h at a dilution of 1/200, plates were washed with PBS/1% Tween 20 and goat anti-mouse IgG1 or IgG2a conjugated to horseradish peroxidase (Southern Biotech Birmingham, AL, USA) was added at 1 μg/ml for 1 h. Plates were again washed and ELISA was developed by *o*-phenylenediamine. Reaction was stopped by 1 M H_2SO_4 and optical density (OD) was read by photometer at 450 nm.

RESULTS

CpG ODN 1826 can be Rapidly Loaded onto Gelatin Nanoparticles

Cationized gelatin nanoparticles of two different diameters (134 nm and ~250 nm) (Table II) were synthesized to

Table II. Sizing Data Obtained by DLS of Unloaded *vs* CpG ODN-Loaded Gelatin Nanoparticles Batches

	Unloaded		Loaded	
	Mean particle size (nm)	PI[a]	Mean particle size (nm)	PI[a]
GNP001	133.8	0.0763	135.3	0.0891
GNP002	244.3	0.0625	245.0	0.0759
GNP003F	232.7	0.0342	233.2	0.0411
GNP004F	255.4	0.0881	259.2	0.0911

n=3
[a] *PI*Polydispersity index

study the impact of particle size on cell uptake and immunostimulation. Compared to the originally described preparation method for gelatin nanoparticles (15), further optimization work was performed. This allows to manufacture highly defined nanoparticles with very narrow size distributions and a predictability of the target size of ±20 nm. The crucial parameters for the later particle size are the amount of gelatin sediment which is redissolved after the first desolvation and the pH value which is adjusted prior the second desolvation step.

All nanoparticle batches utilized were characterized by dynamic light scattering (DLS) with polydispersity indices below 0.1, indicating a high homogeneity in size. An exemplary SEM analysis substantiated the light scattering data and indicated that cationized gelatin nanoparticles prepared by the optimized two-step desolvation procedure are colloidal spheres with a smooth surface morphology (Fig. 1).

Cationization of the nanoparticles was monitored by measuring the ζ potential of the formulations. The linking of cholamine introduces a pH independent cationic net charge onto the nanoparticles due to the quaternary amino group. Consequently, the ζ potentials of all batches were positive independent of the persisting pH conditions, as we previously described (16). After loading of CpG ODN 1826 onto the cationized nanoparticles in PBS of pH 7.4 in a ratio of 1:20 (5% [w/w]), no significant changes, neither in mean size nor in size distribution, were detectable (Table II).

To determine the optimal ODN payload, increasing amounts of CpG ODN 1826 were loaded onto the nanoparticles. After an incubation of 30 min the formulations were analyzed by UV spectroscopy for complete ODN loading. Furthermore, aggregation tendencies were visually monitored and the respective ζ potentials of the formulations were measured in PBS of pH 7.4. Results indicated that up to 100 μg CpG ODN 1826 could be completely loaded onto 600 μg (16.7% [*w*/*w*]) nanoparticles (in 400 μl PBS). However, these nanoparticles were not stable in PBS and tended to aggregate, most probably due to their neutral net charge (Table III) that facilitates aggregation since inter-particulate electrostatic repulsion forces are absent. This aggregation tendency could be circumvented by reducing the amount of payload to 60 μg per 600 μg nanoparticles (10% [*w*/*w*]). In gene therapeutic experiments (16) we have demonstrated that the highest transfection efficiency can be achieved with nanoparticle formulations bearing a final ζ potential of ~+3 mV in PBS of pH 7.4 (conductivity:16–17 mS/cm). Based on these results, 30 μg CpG ODN per 600 μg nanoparticles (5% [*w*/*w*]) were chosen as standard payload for all subsequent *in vitro* experiments, since the respective averaging ζ potentials of the formulations were around this value which was expected to be favorable, e.g. +3.90±0.87 mV for batch GNP002 (Table III).

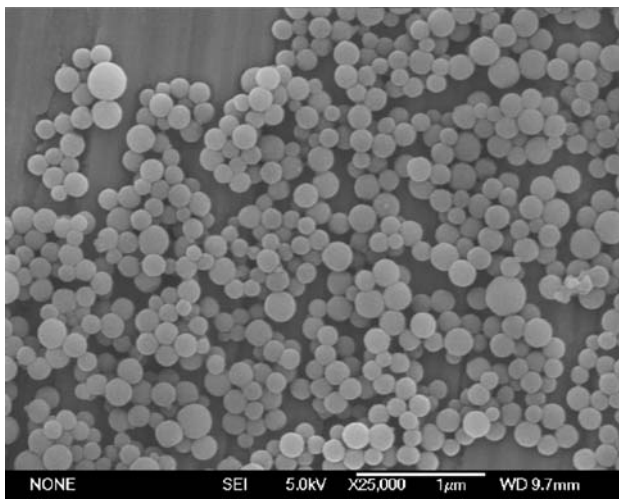

Fig. 1. Scanning electron micrograph of cationized gelatin nanoparticles.

Table III. ζ Potential Values and Visible Aggregation Tendencies of Cationized Gelatin Nanoparticles (batch GNP002) Loaded with Various Amounts of CpG ODN 1826 after 30 min of Incubation

Payload (*w*/*w*)	ζ Potential (conductivity)	Aggregation
Unloaded	+7.39±0.35 mV (17,03 mS/cm)	No
5.0%	+3.90±0.87 mV (16.34 mS/cm)	No
10.0%	+1.33±0.25 mV (16.08 mS/cm)	No
16.7%	−0.63±0.17 mV(17.33 mS/cm)	Yes

Measurements were performed in PBS of pH 7.4; respective conductivity values are in parentheses.

CpG-GNPs are Efficiently Taken up into Murine Myeloid DCs

We have shown in previous studies that unloaded gelatin nanoparticles are efficiently taken up by myeloid DCs (18). To assess the uptake of CpG ODN-loaded cationized gelatin nanoparticles (CpG-GNPs), it was measured by flow cytometry analysis of myeloid DCs incubated for 12 h with CpG ODN 1826-loaded nanoparticles (5% [*w*/*w*]) or with unloaded, non-cationized gelatin nanoparticles (both fluorescence-labeled). The total number of myeloid DCs that had taken up CpG-loaded nanoparticles was 68%, whereas only 33% of the cells had taken up unloaded, non-cationized nanoparticles (Fig. 2).

Although flow cytometry data indicated that CpG ODN-loaded nanoparticles were efficiently taken up by DCs, the localization of these nanoparticles after uptake is unknown. Since internalization of CpG ODN by DCs is required for immunostimulatory activity (19), CLSM studies were employed to pinpoint the intracellular localization of the nanoparticles. Myeloid DCs were positively identified by CD11c antibody. Scanning various planar sections, CpG ODN-loaded and Texas Red-X labeled nanoparticles (GNP003F) were observed as distinct dots within the cells (Fig. 3a). Inhibition of nanoparticle uptake by myeloid DCs following treatment with phagocytosis inhibitor Cytochalasin B indicated that phagocytosis was the main mechanism involved in the nanoparticle uptake process (Fig. 3b).

Cationized Gelatin Nanoparticles Potentiate Immunostimulation of Murine Myeloid DCs by CpG ODN

Following recognition of a danger signal, immature myeloid DCs upregulate surface expression of MHC and co-stimulatory molecules and undergo a maturation process. In the current study, the efficiency of CpG ODN-loaded gelatin nanoparticles in activating myeloid DCs was investigated based on the increase in expression of MHC class II and CD86 molecules. As depicted in Fig. 4, DC cultures treated with CpG-GNPs upregulated surface expression of MHC-II and CD86 molecules. These results indicated that

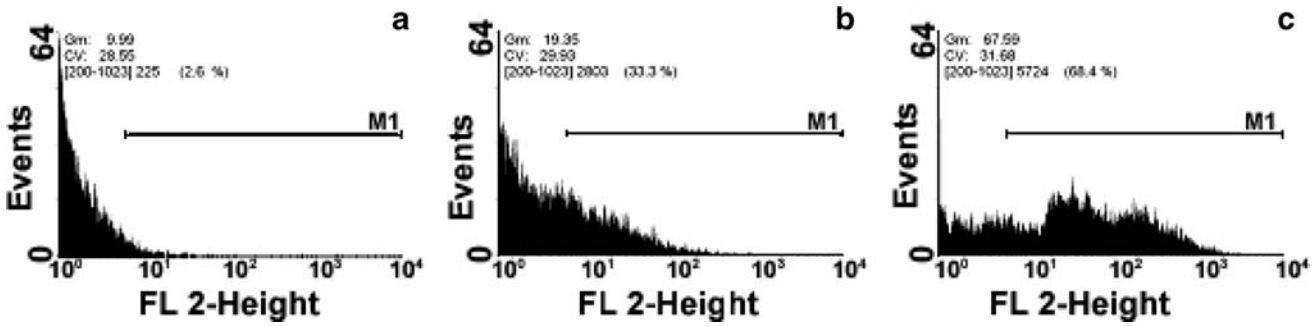

Fig. 2. FACS histogram plots (FL-2 height) of untreated DCs (**a**), DCs incubated with plain non-cationized gelatin nanoparticles (**b**) and DCs incubated with CpG-GNPs (**c**).

delivery of CpG ODN loaded onto cationized gelatin nanoparticles efficiently induced DC maturation.

A preliminary screening by microarray (data not shown) of cytokine production by murine myeloid DCs stimulated with CpG-GNPs suggested that, as is the case with soluble CpG ODNs (20, 21), CpG ODN-loaded gelatin nanoparticles induce a T_H1-type cytokine pattern, whereas unloaded cationized gelatin nanoparticles do not result in cytokine production. Based on these data, quantitative ELISA of IL-12p70, IL-6 and TNF-α secretion were performed after 24 h stimulation of murine myeloid DCs with either free CpG ODN 1826 or CpG ODN-loaded gelatin nanoparticles. In all experiments, no cytokine production was detected in the supernatants of unstimulated cells and of cells treated with either unloaded cationized gelatin nanoparticles or gelatin nanoparticles loaded with non-stimulating ODN (Fig. 5a–c).

The first cytokine quantified was IL-12p70, a key cytokine directing immune responses towards T_H1 (Fig. 5a). While IL-12p70 levels produced by myeloid DCs were 266±53 pg/ml following 24 h stimulation with 10 μg (2 μg/ml) soluble CpG ODN, two different batches of CpG-GNPs were able to induce averages of 595±107 pg/ml (GNP001, 134 nm) and 690±56 pg/ml (GNP0002, 244 nm), demonstrating a two- to threefold cytokine increase by loading CpG ODN onto these nanoparticles. TNF-α, a key inflammatory cytokine that induces DC maturation (22, 23), was secreted in low amounts following soluble CpG ODN treatment whereas CpG ODN loading onto nanoparticles increased secretion seven to nine times (Fig. 5b). As with IL-12p70, the larger sized nanoparticles (GNP0002) resulted in a slightly higher cytokine production. In contrast, no significant difference in IL-6 secretion by murine myeloid DCs was observed following delivery of CpG ODN in nanoparticulate or soluble form (Fig. 5c).

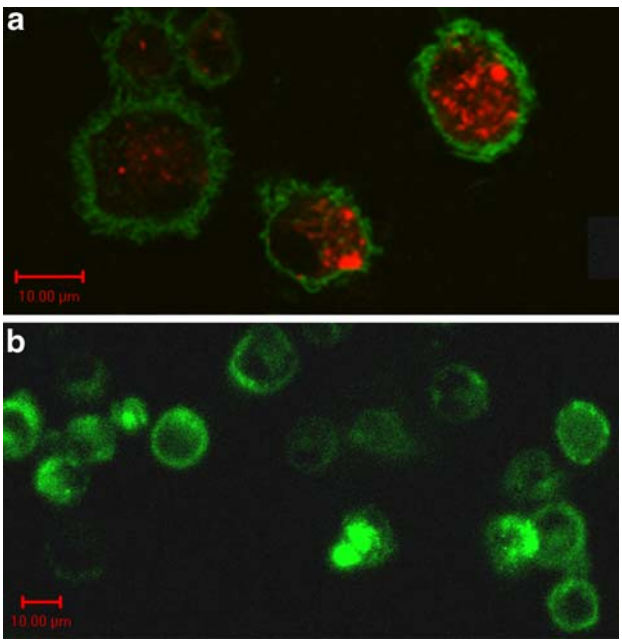

Fig. 3. CLSM images of myeloid DCs (*green*) incubated with CpG-GNPs (*red*) (**a**) and myeloid DCs treated with Cytochalasin B before and during incubation with CpG-GNPs (**b**).

Cationized Gelatin Nanoparticles Increase Immunostimulatory Activity of CpG ODN *In Vivo*

To assess whether CpG ODN bound to cationized gelatin nanoparticles also resulted in immunostimulation *in vivo*, dispersions of CpG ODN 1826 loaded onto two different sized of nanoparticles were injected i.v. into mice (nanoparticle batches: GNPIV1, average size: 289 nm and GNPIV2, average size: 150 nm). For these *in vivo* experiments, the payload of the nanoparticles was increased to 10% (w/w) to keep the amount and volume of nanoparticles (500 mg nanoparticles in 100 μl PBS) to be administered per mice within an acceptable range. 50 μg soluble CpG ODN was injected as positive control. Fig. 6 shows serum levels of the proinflammatory cytokines IL-12p70 (Fig. 6a) and IL-6 (Fig. 6b) 18 h post injection. Both CpG ODN nanoparticulate formulations resulted in elevated levels of both cytokines, whereas unloaded cationized gelatin naoparticles did not induce cytokine production. As seen with *in vitro* stimulation of murine myeloid DCs, the larger sized nanoparticles induced production of proinflammatory cytokines more efficiently. However, the respective differences in immunostimulatory activity between ~150 and ~300 nm sized particles were larger than those seen *in vitro*. 300 nm-sized nanoparticles led to more than threefold higher IL-12p70 concentrations than soluble CpG ODN and to slightly enhanced IL-6 values. In contrast, the 150 nm nanoparticles resulted in IL-12p70 levels similar to soluble CpG ODN, but in reduced secretion of IL-6. No signs of toxicity were observed at any time.

CpG-GNPs do not Induce an Immune Response to Gelatin

Unloaded cationized gelatin nanoparticles did not show immunostimulatory activity *in vitro* nor *in vivo* at any time.

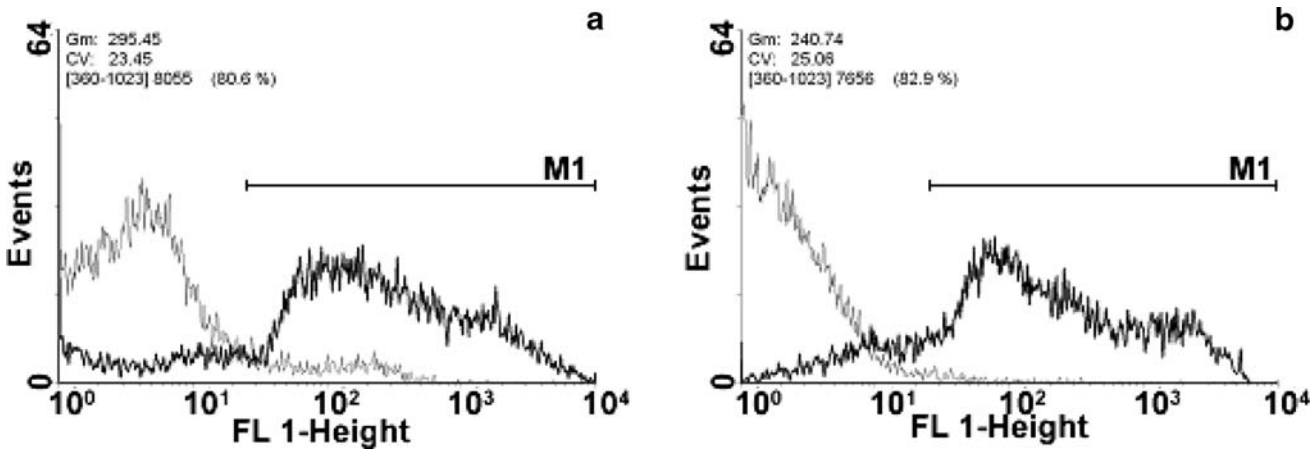

Fig. 4. FACS histogram plots (FL-1 height); MHC II antibody staining (**a**); untreated DCs (*grey*) vs CpG-GNPs (*black*); CD 86 antibody staining (**b**); untreated DCs (*grey*) vs CpG ODN-loaded gelatin nanoparticles (*black*).

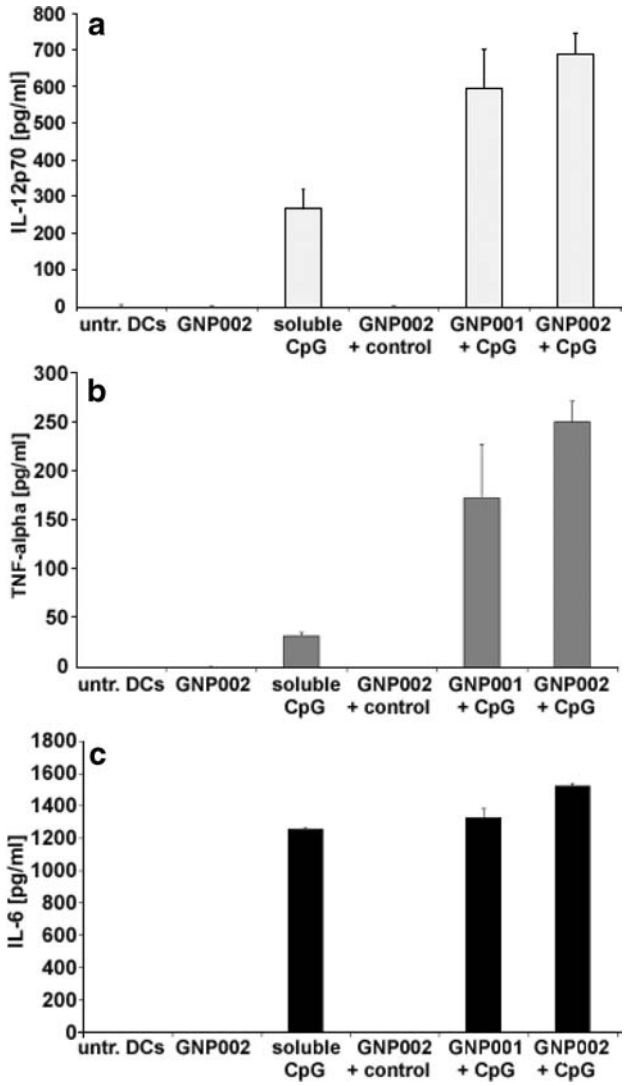

Fig. 5. Levels of IL-12p70 (**a**), TNF-α (**b**), and IL-6 (**c**) per ml cell supernatant after 24 h incubation (n=3): untreated myeloid DCs (untr. DCs); unloaded gelatin nanoparticles GNP002 (GNP002); soluble CpG ODN (soluble CpG); non-stimulating control ODN-loaded gelatin nanoparticles GNP002 (GNP002+control); CpG ODN-loaded gelatin nanoparticles GNP001 (GNP001+CpG); CpG ODN-loaded gelatin nanoparticles GNP002 (GNP002+CpG).

However, the strong T_H1 adjuvant CpG ODN might induce an immune response to the gelatin composing the nanoparticles. To address this issue, serum antibodies to gelatin were assessed in mice having received CpG ODN-loaded gelatin nanoparticles twice at a 14-day interval. Mice immunized with soluble gelatin together with complete Freund's Adjuvant served as positive control. While immu-

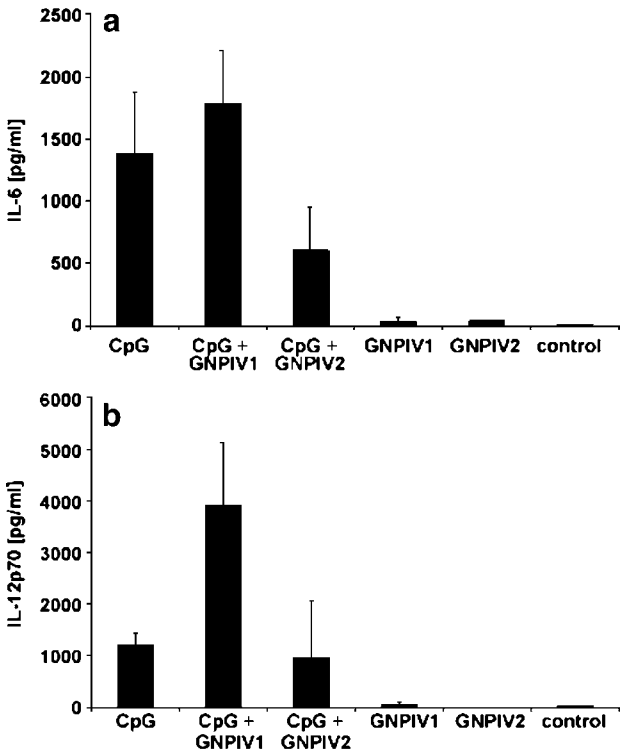

Fig. 6. IL-6 (**a**) and IL-12p70 (**b**) levels per ml blood serum at 18 h postinjection (n=3). CpG: 50 μg soluble CpG ODN; CpG+GNPIV1: 500 μg GNPs (batch GNPIV1: 289 nm) loaded with 50 μg CpG ODN; CpG+GNPIV2: 500 μg GNPs (batch GNPIV2: 150 nm) loaded with 50 μg CpG ODN; GNPIV1/GNPIV2: 500 μg unloaded GNP controls; *control* untreated control mice.

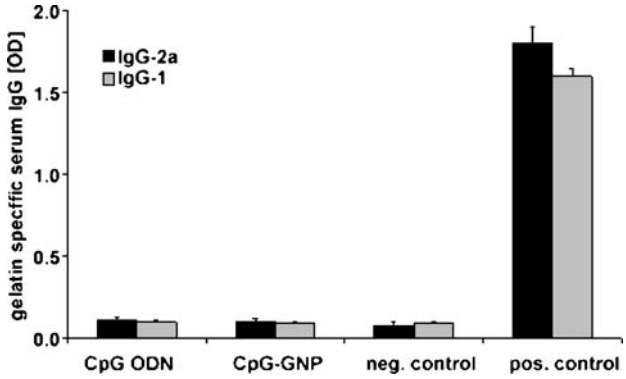

Fig. 7. Serum titers of anti-gelatin IgG of all gelatin nanoparticle samples tested *in vivo* (GNPIV1 and GNPIV2); *CpG ODN* Soluble CpG ODN, *CpG-GNP* CpG ODN-loaded cationized gelatin nanoparticles, *neg. control* PBS, *pos. control* mice treated with gelatin and additional complete Freund's Adjuvant.

nization with gelatin and complete Freund's Adjuvant generated anti-gelatin antibodies of both the IgG1 and IgG2a isotypes, none of the mice injected with CpG ODN-loaded gelatin nanoparticles showed detectable levels of anti-gelatin antibodies after 3 weeks. This indicates that no immune response directed against the proteinaceous matrix material of the carrier system was generated, even following two immunizations with a strong T_H1 adjuvant (Fig. 7).

Gelatin Nanoparticle Loading with Human CpG B and C ODN is Efficient

While CpG ODN bind to both the murine and the human Toll-like receptor 9, resulting in cellular activation and maturation, the optimal CpG motif differs between these two species. To correlate results obtained in the mouse with the human system, loading of nanoparticles with CpG oligonucleotides specific for the human Toll-like receptor 9 was examined. Cationized gelatin nanoparticles were loaded with increasing concentrations of the CpG-A ODN 2216, the CpG-B ODN 2006 or the CpG-C ODN M362. No significant changes in particle size and homogeneity were measured when CpG-B ODN 2006 or CpG-C ODN M362 were used (Table IV). The results were similar to those obtained with the murine CpG-B ODN 1826. No aggregation was detected up to a payload of 10% (*w*/*w*). In contrast, increased aggregation was detected with increasing CpG-A ODN concentrations as early as 30 min after loading. The structure of A-class CpG ODN includes a central palindrome sequence and terminal poly(G) motifs at the 5′ and 3′ end that are capable of forming inter- and intramolecular bonds known as G-tetrads (24). These motifs cause CpG-A ODN to spontaneously form stable nanoparticulate structures under physiological conditions consisting of up to 30 ODN strands (25) with an average mean size of 20–100 nm (26, 27). It is probable that the observed aggregation resulted from adsorption of these colloidal CpG-A particles onto cationized gelatin nanoparticles.

Human Plasmacytoid DCs are Activated by CpG-GNP to Secrete IFN-α

The activation of human cells by cationized gelatin nanoparticles loaded with CpG ODN containing human immunostimulatory motifs was assessed on the two human cell populations that express Toll-like receptor 9 under resting conditions, plasmacytoid dendritic cells and B cells. Two different sizes of nanoparticles were used in order to compare efficacy: GNPH001 (mean size: 160 nm) and GNPH002 (mean size: 293 nm). Identical to murine *in vitro* experiments, the nanoparticles were loaded with CpG ODN at a ratio of 50 μg ODN per mg nanoparticles, i.e. 5% (w/w). The total amount of CpG ODN administered per well either in soluble form or adsorbed onto nanoparticles was 600 ng CpG ODN in 200 μl media (3 μg/ml). Freshly isolated plasmacytoid DCs were incubated with the CpG ODN 2216 (CpG-A), 2006 (CpG-B) and M362 (CpG-C) for 8 h and supernatants were assessed for IFN-α production. While, as previously described, CpG-B did not induce IFN-α secretion by plasmacytoid DCs, adsorption of the CpG ODN 2006 (CpG-B) onto nanoparticles resulted in strong IFN-α production (Fig. 8a).

Soluble CpG-C ODN induced as expected intermediate levels of IFN-α. IFN-α production was increased by particulate administration of CpG-C ODN and even double by formulation with the 293 nm particles. The detected IFN-α production induced by these larger particles were extremely high and even outranged IFN-α induced by soluble CpG-A ODN (ODN 2216), the 'gold-standard' CpG ODN for the induction of IFN-α by plasmacytoid DCs. Interestingly, when plasmacytoid DCs were stimulated with CpG-A ODN loaded onto cationized gelatin nanoparticles, the ability to induce IFN-α was strongly reduced. Incubation of plasmacytoid DCs with nanoparticles loaded with a GpC-control ODN (M383) that does not contain immunostimulatory CpG sequences did not induce cytokine production. This indicates that the

Table IV. DLS Size Determination of Cationized Gelatin Nanoparticles that were Loaded with each CpG ODN Class in Various Payloads

Payload (*w*/*w*)/ODN-Type	CpG-A (ODN 2216)		CpG B (ODN 2006)		CpG C (ODN M362)	
	MPS[a] (nm)	PI[b]	MPS[a] (nm)	PI[b]	MPS[a] (nm)	PI[b]
Unloaded	209.2	0.071	209.2	0.071	209.2	0.071
2.5%	422.7	0.334	208.1	0.101	204.2	0.066
5%	1,203.4	0.667	202.1	0.094	212.1	0.110
7.5%	4,100.6	0.890	201.2	0.087	205.3	0.121
10%	6,475.8	0.875	201.1	0.064	199.9	0.098

Incubation time: 30 min in PBS (n=1);
[a] *MPS*Mean particle size
[b] *PI*Polydispersity index

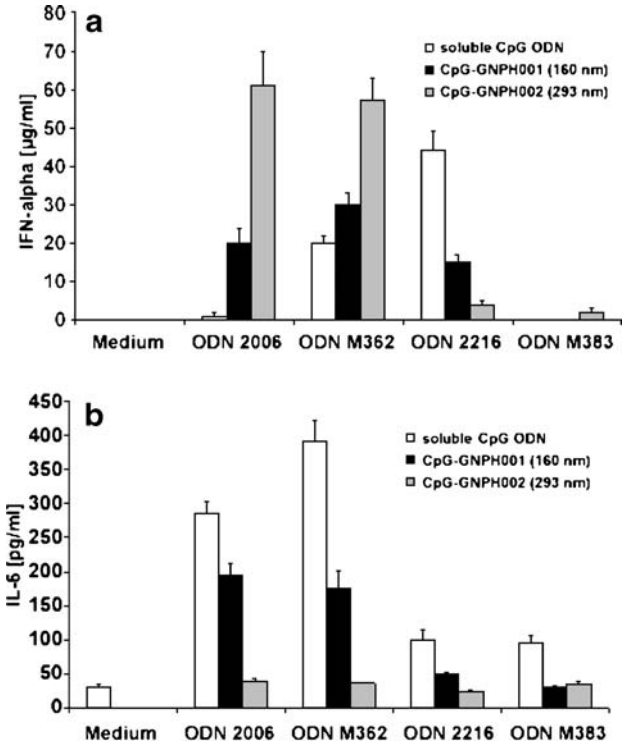

Fig. 8. CpG-GNP induced immunostimulatory activity on plasmacytoid DCs and B cells. Incubation time: 8 h (n=5); applied nanoparticles size: 160 nm (GNPH001) and 300 nm (GNPH002); IFN-α was quantified in the supernatants of DC cultures (**a**); B cells were analyzed for IL-6 (**b**).

presence of CpG motifs is mandatory for the stimulation of the immune system. Furthermore, the nanoparticle formulations showed significant differences in IFN-α induction between the two different sizes of nanoparticles tested. CpG ODN-loaded GNPH002 (293 nm) was far more effective than GNPH001 (160 nm) for cytokine induction in plasmacytoid DCs.

The other human cell population expressing Toll-like receptor 9 in the resting state and thus able to respond directly to CpG ODN stimulation are B cells. The B and C classes of CpG ODN both induce B cell proliferation and rapid secretion of IL-6. We assessed IL-6 production by freshly isolated human B cells upon stimulation with CpG-GNPs as a measure of B cell activation (Fig. 8b). While IL-6 production was stimulated by the soluble forms of both ODN 2006 (CpG-B) and ODN M362 (CpG-C) and to a lesser extent by ODN 2216 (CpG-A), cytokine production was reduced by loading of CpG ODN onto cationized gelatin nanoparticles. In the case of the 293 nm nanoparticle formulation, IL-6 production was completely inhibited. These results indicate that CpG ODN-loaded gelatin nanoparticles do not enhance B cell stimulation compared to soluble CpG ODN. Clearly, particulate presentation of CpG-B and CpG-C promotes activation of Toll-like receptor 9 in plasmacytoid DC, but simultaneously inhibits B cell activation.

CpG-GNPs are Taken up into Human Plasmacytoid DCs

We have demonstrated that particulate presentation of CpG ODN of the classes B and C is beneficial for the induction of IFN-α in plasmacytoid DCs. To examine internalization of CpG ODN bound to cationized gelatin nanoparticles compared to soluble CpG ODN, we performed immunohistochemistry analysis of plasmacytoid DC pre-incubated with fluorescence-labeled CpG ODN either in soluble form or bound to cationized gelatin nanoparticles. We demonstrate that soluble CpG-A ODN 2216, particulate bound CpG-B and soluble CpG-B are all three internalized into plasmacytoid DC. No differences were seen in quantitative uptake of CpG ODN (Fig. 9). Solely, soluble CpG-B

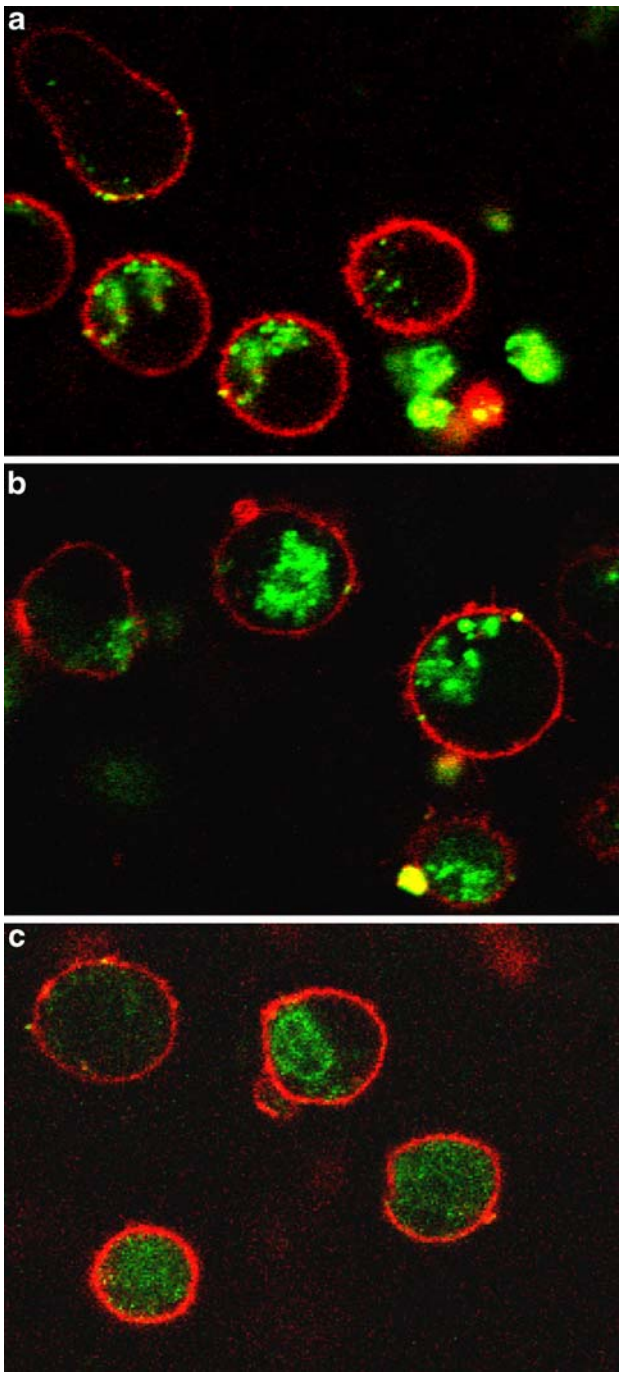

Fig. 9. CLSM images of fluoresceine-labeled CpG ODN uptake into plasmacytoid DCs (2.5×10^5 DCs/ml) after 8 h; administered CpG ODN concentration: 3 µg/ml; soluble CpG ODN 2216 (**a**); CpG ODN 2006 loaded cationized gelatin nanoparticles (**b**); soluble CPG ODN 2006 (**c**).

appears rather diffuse on the images, whereas particulate CpG-B and soluble CpG-A could be identified as distinct dots within plasmacytoid DCs.

DISCUSSION

Professional antigen presenting cells, and dendritic cells (DCs) in particular, naturally phagocytose bacteria, viruses and other microorganisms and process their proteins for antigen presentation to T cells for the induction of antigen-specific immune responses. Colloidal particulate formulations are within the same size range as microorganisms and thus are preferentially phagocytosed by these cells. Hence, particulate vaccine delivery systems have proven to be advantageous for subunit vaccines based on proteins, peptides and DNA (28, 29).

In this study we demonstrate for the first time the use of cationized gelatin nanoparticles as carrier for CpG ODNs. Surface modification with cholamine hydrochloride resulted in the formation of a pH-independent cationic surface charge on the nanoparticles, which should guarantee that no unwanted desorption of the CpG ODN from the carrier surface occurs during the transport to the target cell. A loading ratio of 20:1–10:1 (5–10% [*w*/*w*]) of nanoparticles to CpG ODN was found to be favorable since the formulations remained stable within physiological media and had a slightly positive net charge. According to reports in literature (30–32) positively charged particles are favorable phagocytosed by DCs and macrophages compared to neutral or negatively charged particulate formulations. In agreement with this, murine myeloid DCs internalized the positively charged CpG ODN-loaded cationized gelatin nanoparticles more efficiently than plain non-cationized gelatin nanoparticles (Fig. 2), which have a partially negative ζ potential (16). CLSM studies showed that the uptake of nanoparticles was inhibited by treatment of murine myeloid DCs cultures with Cytochalasin B, an inhibitor of intracellular actin-myosin polymerization, an essential step in phagocytosis (33). Thus, the observed uptake of the cationized gelatin particles by DCs was through active phagocytosis, and neither due to mere adherence of the particles to cell surfaces, nor due to pinocytosis.

We have shown that CpG ODN loaded onto the gelatin nanoparticles upregulate the expression of MHC II and CD86 molecules. This suggests that CpG ODN-loaded gelatin nanoparticles might enhance the immunogenicity of a co-delivered antigen, because the upregulation of MHC and co-stimulatory molecules on the DC surface improves the ability of DCs to activate and prime T cells. Similar to soluble CpG ODN which promotes the secretion of T_H1 polarizing cytokines by DCs (30), CpG ODN-loaded gelatin nanoparticles induced the secretion of the proinflammatory cytokines both *in vitro* and *in vivo*. The extent of secretion of IL-12p70 and TNF-α induced by CpG-GNPs was however increased in comparison to that observed for soluble CpG ODN.

Regarding particle size, the larger sized batch GNP0002 (245 nm) induced slightly higher immune stimulation than GNP0001, having a mean size of 135 nm. This finding is in agreement with Foged *et al.* (32), who tested the phagocytosis activity of various polystyrene particles in a diameter range between 0.04–15 μm and found that particle diameters around 0.5 μm and slightly below were optimal for uptake into DCs. Importance of nanoparticle size for induction of cytokine secretion was even pronounced during *in vivo* experiments, where ~300 nm sized nanoparticles showed better results than ~150 nm sized. The uptake of CpG ODN into the endosomal compartment by phagocytic cells is essential to induce cytokine production. The uptake of larger particles (>200 nm) results in longer retention of particulate material in the endosomal vesicles (34). This may increase signaling by CpG-ODN via the endosomal Toll-like receptor 9, thereby leading to sustained cell activation and IFN-α production (35).

Safety of carrier formulations is essential to justify the further development of CpG ODN-loaded gelatin nanoparticles. The absence of cytokine secretion following treatment of myeloid DC cultures with unloaded nanoparticles or control, non-stimulatory ODN indicated endotoxin-free conditions of the preparation process, as even low levels of endotoxin contamination would have triggered cytokine secretion by DCs. In developing carriers for nucleic acids, a major concern is the possible development of an immune response against the carrier that would render subsequent applications of the same carrier ineffective. In this study we show that the application of CpG ODN-loaded gelatin nanoparticles does not result in the generation of an antigen-specific immune response to gelatin, the matrix material of the nanoparticles. These data are already very promising and give a certain hint that cationized gelatin nanoparticles are not immunogenic at all. However, for final clarification this topic will also be an important point in future experimental setups.

Experiments in primary human plasmacytoid DCs confirmed the enhanced activation through CpG ODN formulations when delivered with gelatin nanoparticles. Regarding the various classes of CpG ODNs for humans, we were able to show that the structural prerequisites for the successful presentation of CpG ODNs to B cells and plasmacytoid DCs differ remarkably. Comparable IFN-α levels with CpG-B and CpG-C adsorbed onto the surface of cationized gelatin nanoparticles suggest that the activation of plasmacytoid DCs is driven by the nanoparticulate structure rather than a specific sequence. These findings are in agreement with the results of other research groups using cationic PLGA microparticles (36) or microparticles based on the polycationic antibiotic polymyxin B (37). Adsorption of CpG-A ODN 2216 on nanoparticles, which already possesses a particulate structure, led to large aggregates which cannot be internalized into plasmacytoid DCs and/or act as signal transducer.

Other groups have described that multimeric presentation induces cross-linking of TLR9 in plasmacytoid DCs, thus leading to the enhanced secretion of IFN-α. In contrast, soluble monomeric CpG-B ODN fails to induce significant IFN-α secretion (36–38). Presumably, the presentation of CpG ODN as particulate matter allows various receptor–ligand interactions and amplifies the transcription of IFN-α. Thus, an optimized primary sequence for immune stimulation of plasmacytoid DCs such as the ODN 2216 sequence (palindrome, chimeric backbone, poly-G ends) is not mandatory. CpG-B ODN 2006 attached onto gelatin nanoparticles revealed even better immunogenic activation patterns. The specific ODN sequence of CpG-A is required to form a particulate structure of the CpG ODN by self-assembly, but the recognition by TLR9 occurs by the CpG motif alone.

In contrast, the activation of B cells seems mainly to be driven by the sequence of the CpG ODN, whereas particulate delivery appears to be rather disadvantageous. However, particulate-bound CpG-B ODN 2006 and CpG-C ODN M362 are still able to activate B cells. Apparently, the respective degree of B cell activation depends on the size of the utilized nanoparticles. Nevertheless, the present data demonstrate that optimized activation of B cells and plasmacytoid DCs requires completely different delivery and presentation of CpG ODN. Possible explanations for these differences might be that polymorphic types of TLR9 do exist in plasmacytoid DCs and B cells, which require different structural prerequisites of their particular ligands, or that a non-identified CpG co-receptor exists in one of the two cell populations, or alternatively that TLR9 is located in different compartments of the endosome with different accessibility and activation requirements.

In addition to the recognition of CpG ODN by Toll-like receptor 9, recent reports have shown that nucleic acids from pathogens are recognized by several other receptors of the innate immune system. In particular, the 5′-triphosphate end of RNA generated by viral polymerases directly binds to RIG-I (39). Single-stranded viral RNA and immunostimulatory oligoribonucleotides are detected through TLR7 and TLR8 and can induce T_H1-type immunity (40–42). These RNA-based molecular danger signals may equally benefit from the carrier function of cationic gelatin nanoparticles for therapeutic applications.

CONCLUSION

Cationized gelatin nanoparticles have demonstrated to be a highly valuable carrier system for immunogenic CpG ODNs. In summary, CpG-GNP formulations of CpG-B ODN 2006 and CpG-C ODN M362 represent a promising alternative to CpG-A ODN 2216 for the selective endogenous secretion of IFN-α. The formulation presented in this study would enable a dose reduction of CpG ODN or binding of novel RNA-based adjuvants for therapeutic use. The protein-based structure of gelatin offers a multitude of functional groups that would allow additional linkage of an antigen. Thus, all-in-one vaccine formulations containing both antigen and immunostimulatory oligonucleotides as adjuvant may be applied against cancer or viral infections.

ACKNOWLEDGMENTS

The author would like to dedicate this article to Prof. Dr. John Samuel, who passed away far too soon. We thank him and Praveen Elamanchili from the Faculty of Pharmacy at the University of Alberta for their awesome support during the first experiments with CpG ODNs. We thank Nadja Sandholzer for expert technical assistance. This study was supported by grants BMBF Biofuture 0311896 to G.H., and from the Else-Kröner Fresenius Foundation and the German Research Foundation (DFG En 169/7-2 and GK 1202) to C.B. and S.E.

REFERENCES

1. A. M. Krieg. Therapeutic potential of Toll-like receptor 9 activation. *Nat. Rev., Drug Discov.* **5**(6):471–484 (2006).
2. M. Diwan, M. Tafaghodi, and J. Samuel. Enhancement of immune responses by co-delivery of a CpG oligodeoxynucleotide and tetanus toxoid in biodegradable nanospheres. *J. Control. Release* **85**(1–3):247–262 (2002).
3. M. Diwan, P. Elamanchili, M. Cao, and J. Samuel. Dose sparing of CpG oligodeoxynucleotide vaccine adjuvants by nanoparticle delivery. *Curr. Drug Deliv.* **1**(4):405–412 (2004).
4. S. Jain, W. T. Yap, and D. J. Irvine. Synthesis of protein-loaded hydrogel particles in an aqueous two-phase system for coincident antigen and CpG oligonucleotide delivery to antigen-presenting cells. *Biomacromolecules* **6**(5):2590–2600 (2005).
5. Y. J. Kwon, S. M. Standley, S. L. Goh, and J. M. J. Frechet. Enhanced antigen presentation and immunostimulation of dendritic cells using acid-degradable cationic nanoparticles. *J. Control. Release* **105**(3):199–212(2005).
6. M. Singh, G. Ott, J. Kazzaz, M. Ugozzoli, M. Briones, J. Donnelly, and D. T. O'Hagan. Cationic microparticles are an effective delivery system for immune stimulatory CpG DNA. *Pharm. Res.* **18**(10):1476–1479 (2001).
7. Y. Suzuki, D. Wakita, K. Chamoto, Y. Narita, T. Tsuji, T. Takeshima, H. Gyobu, Y. Kawarada, S. Kondo, S. Akira, H. Katoh, H. Ikeda, and T. Nishimura. Liposome-encapsulated CpG oligodeoxynucleotides as a potent adjuvant for inducing type 1 innate immunity. *Cancer Res.* **64**(23):8754–8760 (2004).
8. A. Joseph, I. Louria-Hayon, A. Plis-Finarov, E. Zeira, Z. Zakay-Rones, E. Raz, T. Hayashi, K. Takabayashi, Y. Barenholz, and E. Kedar. Liposomal immunostimulatory DNA sequence (ISS-ODN): an efficient parenteral and mucosal adjuvant for influenza and hepatitis B vaccines. *Vaccine* **20**(27–28):3342–3354 (2002).
9. R. Rankin, R. Pontarollo, X. Ioannou, A. M. Krieg, R. Hecker, L. A. Babiuk, and Littel-van den Hurk van Drunen, S. CpG motif identification for veterinary and laboratory species demonstrates that sequence recognition is highly conserved. *Antisense Nucleic Acid Drug Dev.* **11**(5):333–340 (2001).
10. G. Hartmann, and A. M. Krieg. Mechanism and function of a newly identified CpG DNA motif in human primary B cells. *J. Immunol.* **164**(2):944–953 (2000).
11. S. Rothenfusser, E. Tuma, S. Endres, and G. Hartmann. Plasmacytoid dendritic cells: the key to CpG. *Hum. Immunol.* **63**(12):1111–1119 (2002).
12. G. Hartmann, J. Battiany, H. Poeck, M. Wagner, M. Kerkmann, N. Lubenow, S. Rothenfusser, and S. Endres. Rational design of new CpG oligonucleotides that combine B cell activation with high IFN-α induction in plasmacytoid dendritic cells. *Eur. J. Immunol.* **33**(6):1633–1641 (2003).
13. A. G. Ward, and A. Courts. *The Science and Technology of Gelatin*. Academic Press, New York, 1977.
14. H. G. Schwick, and K. Heide. Immunochemistry and immunology of collagen and gelatin. *Bibl. Haematol.* **33**:111–125 (1969).
15. C. Coester, H. von Briesen, K. Langer, and J. Kreuter. Gelatin nanoparticles by two step desolvation—a new preparation method, surface modifications and cell uptake. *J. Microencapsul* **17**:187–194 (2000).
16. K. Zwiorek, J. Kloeckner, E. Wagner, and C. Coester. Gelatin nanoparticles as a new and simple gene delivery system. *J. Pharm. Pharm. Sci.* **7**(4):22–28 (2004).
17. M. B. Lutz, N. Kukutsch, A. L. Ogilvie, S. Rossner, F. Koch, N. Romani, and G. Schuler. An advanced culture method for generating large quantities of highly pure dendritic cells from mouse bone marrow. *J. Immunol. Methods* **223**(1):77–92 (1999).
18. C. Coester, P. Nayyar, and J. Samuel. *In vitro* uptake of gelatin nanoparticles by murine dendritic cells and their intracellular localisation. *Eur. J. Pharm. Biopharm.* **62**(3):306–314 (2006).
19. A. M. Krieg, A. K. Yi, S. Matson, T. J. Waldschmidt, G. A. Bishop, R. Teasdale, G. A. Koretzky, and D. M. Klinman. CpG motifs in bacterial DNA trigger direct B-cell activation. *Nature* **374**(6522):546–549 (1995).
20. A. M. Krieg. CpG motifs in bacterial DNA and their immune effects. *Annu. Rev. Immunol.* **20**:709–760 (2002).
21. T. Jakob, P. S. Walker, A. M. Krieg, E. Von Stebut, M. C. Udey, and J. C. Vogel. Bacterial DNA and CpG-containing oligodeoxynucleotides activate cutaneous dendritic cells and induce IL-12 production: implications for the augmentation of Th1 responses. *Int. Arch. Allergy Immunol.* **118**(2–4):457–461 (1999).

22. J. F. Arrighi, M. Rebsamen, F. Rousset, V. Kindler, and C. Hauser. A critical role for p38 mitogen-activated protein kinase in the maturation of human blood-derived dendritic cells induced by lipopolysaccharide, TNF-a, and contact sensitizers. *J. Immunol.* **166**(6):3837–3845 (2001).
23. N. Iijima, Y. Yanagawa, and K. Onoe. Role of early- or late-phase activation of p38 mitogen-activated protein kinase induced by tumour necrosis factor-a or 2,4-dinitrochlorobenzene during maturation of murine dendritic cells. *Immunology* **110**(3):322–328 (2003).
24. A. Krug, S. Rothenfusser, V. Hornung, B. Jahrsdorter, S. Blackwell, Z. K. Ballas, S. Endres, A. M. Krieg, and G. Hartmann. Identification of CpG oligonucleotide sequences with high induction of IFN-a/b in plasmacytoid dendritic cells. *Eur. J. Immunol.* **31**:2154–2163 (2001).
25. J. D. Marshall, K. Fearon, C. Abbate, S. Subramanian, P. Yee, J. Gregorio, R. L. Coffman, and G. Van Nest. Identification of a novel CpG DNA class and motif that optimally stimulate B cell and plasmacytoid dendritic cell functions. *J. Leukoc. Biol.* **73**(6):781–792 (2003).
26. L. T. Costa, M. Kerkmann, G. Hartmann, S. Endres, P. M. Bisch, W. M. Heckl, and S. Thalhammer. Structural studies of oligonucleotides containing G-quadruplex motifs using AFM. *Biochem. Biophys. Res. Commun.* **313**(4):1065–1072 (2004).
27. M. Kerkmann, L. T. Costa, C. Richter, S. Rothenfusser, J. Battiany, V. Hornung, J. Johnson, S. Englert, T. Ketterer, W. Heckl, S. Thalhammer, S. Endres, and G. Hartmann. Spontaneous formation of nucleic acid-based nanoparticles is responsible for high interferon-a induction by CpG-A in plasmacytoid dendritic cells. *J. Biol. Chem.* **280**(9):8086–8093 (2005).
28. S. Raychaudhuri, and K. L. Rock. Fully mobilizing host defense: building better vaccines. *Nat. Biotechnol.* **16**(11):1025–1031 (1998).
29. M. Singh, and D. T. O'Hagan. Recent advances in vaccine adjuvants. *Pharm. Res.* **19**(6):715–728 (2002).
30. L. Thiele, B. Rothen-Rutishauser, S. Jilek, H. Wunderli-Allenspach, H. P. Merkle, and E. Walter. Evaluation of particle uptake in human blood monocyte-derived cells *in vitro*. Does phagocytosis activity of dendritic cells measure up with macrophages? *J. Control. Release* **76**(1–2):59–71 (2001).
31. M. Roser, and T. Kissel. Surface-modified biodegradable albumin nano- and microspheres. Part 1. Preparation and characterization. *Eur. J. Pharm. Biopharm.* **39**(1):8–12 (1993).
32. C. Foged, B. Brodin, S. Frokjaer, and A. Sundblad. Particle size and surface charge affect particle uptake by human dendritic cells in an *in vitro* model. *Int. J. Pharm.* **298**(2):315–322 (2005).
33. A. T. Davis, R. Estensen, and P. G. Quie. Cytochalasin B. 3. Inhibition of human polymorphonuclear leukocyte phagocytosis. *Proc. Soc. Exp. Biol. Med.* **137**(1):161–164 (1971).
34. J. M. Brewer, K. G. Pollock, L. Tetley, and D. G. Russell. Vesicle size influences the trafficking, processing, and presentation of antigens in lipid vesicles. *J. Immunol.* **173**(10):6143–6150 (2004).
35. K. Honda, Y. Ohba, H. Yanai, H. Negishi, T. Mizutani, A. Takaoka, C. Taya, and T. Taniguchi. Spatiotemporal regulation of MyD88-IRF-7 signalling for robust type-I interferon induction. *Nature* **434**:1035–1040 (2005).
36. K. Fearon, J. D. Marshall, C. Abbate, S. Subramanian, P. Yee, J. Gregorio, G. Teshima, G. Ott, S. Tuck, G. Van Nest, and R. L. Coffman. A minimal human immunostimulatory CpG motif that potently induces IFN-g and IFN-a production. *Eur. J. Immunol.* **33**(8):2114–2122 (2003).
37. J. D. Marshall, D. Higgins, C. Abbate, P. Yee, G. Teshima, G. Ott, T. dela Cruz, D. Passmore, K. L. Fearon, S. Tuck, and G. Van Nest. Polymyxin B enhances ISS-mediated immune responses across multiple species. *Cell. Immunol.* **229**(2):93–105 (2004).
38. C. C. N. Wu, J. Lee, E. Raz, M. Corr, and D. A. Carson. Necessity of oligonucleotide aggregation for toll-like receptor 9 activation. *J. Biol. Chem.* **279**(32):33071–33078 (2004).
39. V. Hornung, J. Ellegast, S. Kim, K. Brzózka, A. Jung, H. Kato, H. Poeck, S. Akira, K.-K. Conzelmann, M. Schlee, S. Endres, and G. Hartmann. 5′-Triphosphate RNA Is the Ligand for RIG-I. *Science* **314**(5801):994–997 (2006).
40. S. S. Diebold, T. Kaisho, H. Hemmi, S. Akira, and C. Reis e Sousa. Innate antiviral responses by means of TLR7-mediated recognition of single-stranded RNA. *Science* **303**(5663):1529–1531 (2004).
41. V. Hornung, M. Guenthner-Biller, C. Bourquin, A. Ablasser, M. Schlee, S. Uematsu, A. Noronha, M. Manoharan, S. Akira, A. de Fougerolles, S. Endres, and G. Hartmann. Sequence-specific potent induction of IFN-alpha by short interfering RNA in plasmacytoid dendritic cells through TLR7. *Nat. Med.* **11**(3):263-270 (2005).
42. C. Bourquin, L. Schmidt, V. Hornung, C. Wurzenberger, D. Anz, N. Sandholzer, S. Schreiber, A. Voelkl, G. Hartmann, and S. Endres. Immunostimulatory RNA oligonucleotides trigger an antigen-specific cytotoxic T cell and IgG2a response. *Blood* **109**:2953–2960 (2007).